DOI: 10.12923/cipms-2026-0005 Curr. Issues Pharm. Med. Sci., Vol. 39, No. 1, Pages 26-33

Current Issues in Pharmacy and Medical Sciences
Formerly ANNALES UNIVERSITATIS MARIAE CURIE-SKLODOWSKA, SECTIO DDD, PHARMACIA

journal homepage: https://czasopisma.umlub.pl/curipms

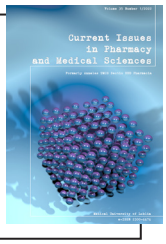

Evaluation of ZnO nanoparticles biosynthesized from *Camellia sinensis* leaves: Anticancer effects on HepG2 cells, antioxidant activity, and anti-hemolytic properties

Halah Al-Luhaiby[1], Jabbar Abadi Mohammed[2*]

[1] Department of Physiology and Medical Physics, Faculty of Medicine, Jabir ibn Hayyan University for Medical and Pharmaceutical Sciences, Kufa, Iraq
[2] Department of Biology, Faculty of Science, University of Kufa, Iraq

ARTICLE INFO

Received 17 May 2024
Accepted 22 December 2025

Keywords:
ZnO nanoparticles;
anticancer activity;
Camellia sinensis;
HepG2 cells;
antioxidant activity;
antihemolytic properties.

ABSTRACT

Hepatocellular carcinoma (HCC) is the most common primary liver cancer and represents a major global health burden due to its high incidence, limited treatment options, and negative impact on patient quality of life. This study aimed to evaluate the anticancer potential of green-synthesized zinc oxide nanoparticles (ZnO NPs) as a natural alternative therapeutic strategy against HCC. ZnO NPs were biosynthesized using *Camellia sinensis* leaf extract. The cytotoxic activity of ZnO NPs against human hepatocellular carcinoma cells (HepG2) was assessed using the MTT assay following 72 hours of treatment. Antioxidant activity was determined using the DPPH free radical scavenging assay. Hemocompatibility was evaluated using an erythrocyte hemolysis assay, while genotoxic effects were examined using a DNA fragmentation assay. ZnO NPs exhibited a significant, concentration-dependent cytotoxic effect on HepG2 cells. Cell viability decreased to 42.13% at 0.5 µg/mL and 26.84% at 5 µg/mL after 72 hours of exposure. The IC_{50} value was calculated as 2.87 µg/mL, indicating strong antiproliferative activity at low concentrations. Antioxidant analysis revealed enhanced free radical scavenging activity with increasing ZnO NP concentrations, reaching a maximum of 81.63% at 1 µg/mL and a minimum of 63.73% at 0.12 µg/mL. Hemolysis levels remained below detectable limits at all tested concentrations (0.12-1 µg/mL), demonstrating excellent hemocompatibility. Moreover, ZnO NPs did not induce DNA fragmentation, confirming the preservation of DNA integrity. The findings of this study demonstrate that ZnO NPs possess significant anticancer activity at low concentrations while exhibiting excellent hemocompatibility and no detectable DNA damage *in vitro*.

INTRODUCTION

Hepatocellular carcinoma (HCC) is the most prevalent form of primary liver cancer and represents a highly aggressive malignancy that can be fatal if not detected at an early stage. In Iraq, most liver cancer cases occur in individuals between 50 and 61 years of age [1]. Effective management of HCC requires early detection and accurate diagnosis, followed by an individualized treatment plan that may include immunotherapy, targeted therapy, surgical resection, or liver transplantation, depending on disease stage and severity [2]. However, these treatments are often associated with major limitations, such as cancer cell resistance, damage to healthy tissues, toxic effects on normal cells, poor target specificity, and destruction of healthy cells at levels comparable to or greater than cancer cell destruction. Moreover, high therapeutic doses may cause a wide range of adverse effects and long-term complications, further limiting their overall effectiveness [3-7].

Consequently, growing interest has emerged in developing natural, safer, and more cost-effective therapeutic alternatives for managing various diseases, including cancer. Advances in modern biomedical research have highlighted the potential role of nanoparticles, herbal compounds, and complementary medicine in cancer diagnosis and therapy. Plant-derived secondary metabolites and natural antioxidants demonstrate potent free radicalscavenging activity,

* **Corresponding author**
e-mail: jabbar.alaridi@uokufa.edu.iq, halah.f.hasan@jmu.edu.iq

which can mitigate oxidative stress, a major contributor to carcinogenesis, thereby offering protective or therapeutic benefits [8,9]. Numerous in vitro and in vivo studies have also reported that green tea (*Camellia sinensis*) exhibits strong anticancer properties, helping to inhibit tumor initiation, progression, and metastasis in several cancer types, including prostate, bladder, breast, liver, and gastrointestinal cancers [6,10].

Furthermore, combining plant extracts with nanoparticles has shown promising advantages over conventional treatments by enhancing biological compatibility, improving targeted delivery, and reducing systemic toxicity [11,12]. The rapidly advancing field of nanotechnology has significantly contributed to the development of novel cancer therapies. Over recent decades, a wide range of nanomaterials has been evaluated in clinical trials to assess their therapeutic efficacy and safety profiles [12]. Nanoparticles (1-100 nm) possess unique characteristics, such as biocompatibility, low toxicity, structural stability, enhanced permeability and retention effects, and improved targeting accuracy, that make them ideal candidates for cancer treatment. They can be classified into several groups, including carbonbased nanoparticles, organic nanoparticles, metalbased nanoparticles, and composite nanoparticles. Importantly, nanoparticlemediated drug delivery systems consider both tumor microenvironment characteristics and physicochemical factors, enabling improved therapeutic outcomes and helping overcome various mechanisms of drug resistance [13,14].

Mineral oxides (MOs) have multiple biomedical applications, including use in biosensors, targeted drug and gene delivery, antimicrobial activity, anticancer therapy, and cellular imaging [15]. Among them, zinc oxide nanoparticles (ZnO NPs) have attracted significant attention due to their selective cytotoxicity toward cancer cells while maintaining low toxicity toward healthy cells. These properties make ZnO NPs promising candidates for cancer diagnosis and treatment, as well as for a variety of other bio-based applications [16,17].

MATERIALS AND METHODS

Leaves of the *Camellia sinensis* plant were purchased from a local market in Najaf, Iraq. The leaves were washed thoroughly with tap water to remove debris and prevent microbial growth. They were then air-dried at room temperature for ten days with occasional manual stirring to ensure uniform drying. After complete drying, the leaves were ground into a fine powder using an electric milling machine.

ZnO nanoparticles (ZnO NPs) were synthesized with slight modifications to the method described in [18]. Briefly, 20 g of green tea leaf powder was mixed with 400 mL of distilled water in a 500 mL glass beaker and heated on a magnetic stirrer at 80°C and 200 rpm for 15 minutes. After heating, the mixture was allowed to cool. For every 100 mL of the aqueous extract, 0.2 g of pure zinc acetate [$Zn(CH_3CO_2)_2 \cdot H_2O$] was added. To adjust the pH to neutral, sodium hydroxide (NaOH) was added dropwise while observing the color change and formation of a white precipitate, indicating the synthesis of ZnO NPs. The mixture was then stirred continuously on a magnetic stirrer for 24 hours to ensure uniform nanoparticle formation.

The formation of ZnO NPs was confirmed spectrophotometrically by measuring the absorbance wavelength of the sample. A maximum absorbance peak at 360.093 nm was recorded, consistent with the characteristic optical properties of ZnO nanoparticles. The mixture was then filtered using Whatman No. 1 filter paper, and the filtrate was collected.

To remove impurities, the filtrate was centrifuged using a cooling centrifuge at 4500 rpm for 30 minutes. The resulting pellet was washed with distilled water and mixed thoroughly using a vortex mixer until fully dispersed. This washing and centrifugation process was repeated three times to obtain a clear supernatant and purified sediment. The final sediment containing ZnO NPs was dried in an oven at 45°C until complete dehydration. The dried ZnO NPs were stored in airtight containers until characterization tests were performed, including X-ray diffraction (XRD), to confirm nanoparticle formation and structural properties.

X-ray Diffraction (XRD) analysis

X-ray diffraction (XRD) was used to characterize the crystal structure of the ZnO nanoparticles. The analysis was conducted at the Research Center, University of Tehran, Iran. XRD provides information on the average crystallite size, structural composition, crystallinity, and phase purity of nanoparticles [19].

The dried ZnO NP sample was placed on a clean glass slide for analysis. XRD measurements were performed at a current of 30 mA and a voltage of 40 kV. The diffraction pattern obtained was used to confirm the successful synthesis and crystalline structure of the ZnO NPs.

Cell culture

The HepG2 cell line (human hepatocellular carcinoma) was obtained from the Exir Research Center. Cells were cultured following standard cell bank protocols using complete RPMI-1640 medium. The complete medium contained RPMI-1640 supplemented with 10% fetal bovine serum (FBS), 1% penicillin-streptomycin (100 U/mL), and 1% Lglutamine.

Cells were maintained in Tflasks and incubated at 37°C in a humidified atmosphere containing 5% CO_2. Cell growth and proliferation were monitored regularly, and cells were used for experiments once they reached 70-80% confluence [20].

Determination of cell proliferation (MTT assay)

The effect of ZnO nanoparticles biosynthesized from *C. sinensis* leaves on HepG2 cell proliferation was assessed using the MTT assay. Cell viability was measured using the methylthiazolyltetrazolium (MTT) reagent prepared by dissolving 50 mg of MTT powder in 10 mL of phosphate-buffered saline (PBS).

HepG2 cells were seeded in 96well plates at a density of 500-10,000 cells per well in 200 µL of complete RPMI-1640 medium. After 24 hours of incubation, a uniform monolayer was formed. Cells were then treated with ZnO NP concentrations of 0, 0.5, 1, 2, and 5 µg/mL. Treated and untreated control cells were incubated for 72 hours at 37°C.

Following incubation, 150 µL of fresh medium and 50 µL of MTT solution (2 mg/mL in PBS) were added to each well. Plates were incubated for an additional 4 hours at 37°C to allow formation of formazan crystals. After incubation, the MTTcontaining medium was carefully removed, and 200 µL of dimethyl sulfoxide (DMSO) along with 25 µL of Sorenson's glycine buffer (0.1 M glycine, 0.1 M NaCl, pH 10.5) were added to each well to dissolve the crystals.

Absorbance was measured at 570 nm using a microplate reader [21]. Cell viability was calculated according to the following formula:

$$\% \text{ Cell viability} = \frac{\text{OD Sample}}{\text{OD cell control}} \times 100\%,$$

where OD represents Optical Density.

Antioxidant activity (DPPH free radical scavenging assay)

The antioxidant activity of ZnO nanoparticles was evaluated using a modified method described in [22]. A stock DPPH solution was prepared by dissolving 6 mg of 1,1diphenyl2picrylhydrazyl (DPPH) in 100 mL of methanol. ZnO NPs were tested at concentrations of 0.12, 0.25, 0.5, and 1 µg/mL.

For each concentration, 100 µL of the DPPH solution was mixed with 100 µL of the nanoparticle sample in a 96well microplate. The plate was incubated in the dark at room temperature for 30 minutes to allow the reaction to occur. After incubation, the absorbance was measured at 517 nm using an ELISA microplate reader. Methanol (200 µL) was used as the blank, while 200 µL of DPPH solution served as the control.

The DPPH radical scavenging activity was calculated using the formula:

$$\text{DPPH scavenging activity (\%)} = \frac{A_0 - A_1}{A_0} \times 100$$

where:
A_0 = absorbance of control
A_1 = absorbance of standard

Effects of ZnO nanoparticles on hemolysis

The hemolytic activity of ZnO NPs was assessed using a modified protocol based on reference [23]. Fresh whole blood was collected from healthy donors, and 285 µL of whole blood was transferred into six Eppendorf tubes. Triton X100 (15 µL of a decomposed solution) was added as the positive control, while phosphate-buffered saline (PBS) was used as the negative control.

For the test samples, 15 µL of each ZnO NP concentration (0.12, 0.25, 0.5, and 1 µg/mL) was added to the tubes containing blood. All samples were incubated in a shaking incubator at 37°C for 2-4 hours. After incubation, the tubes were centrifuged at 8000 rpm for 5 minutes to separate plasma from blood cells.

The supernatant was transferred to a 96well microplate, and absorbance was measured at 492 nm using an ELISA plate reader. The percentage of hemolysis was calculated using the equation:

$$H\ (\%) = \frac{OD_{550nm}\ \text{sample} - OD_{550nm}\ \text{negative}}{OD_{550nm}\ \text{positive} - OD_{550nm}\ \text{negative}} \times 100,$$

where OD represents Optical Density.

DNA fragmentation test

The potential genotoxic effects of ZnO nanoparticles were evaluated using a DNA fragmentation assay following a modified protocol described in [24]. Human genomic DNA was used instead of bacterial DNA to assess the direct impact of ZnO NPs on eukaryotic DNA integrity.

ZnO NPs were tested at concentrations of 0.125, 0.250, 0.500, and 1 µg/mL. For each treatment, 100 µL of the nanoparticle suspension was mixed with 100 µL of DNA solution. A control sample was prepared by mixing 100 µL of distilled water with 100 µL of DNA.

All samples were incubated for 2 hours at 37°C in saline solution, maintaining phosphate buffering capacity using PBS at pH 7.4. After incubation, samples were prepared for agarose gel electrophoresis to evaluate any structural changes or fragmentation in the DNA.

Agarose gel electrophoresis

Agarose gel electrophoresis was used to analyze DNA integrity following nanoparticle treatment. The procedure was performed according to the method in [25], with minor modifications.

A 1% agarose gel was prepared by dissolving 1 g of agarose powder in 100 mL of 1× TrisborateEDTA (TBE) buffer. The mixture was heated in a microwave until the agarose was fully dissolved. After cooling to 50-55°C, ethidium bromide was added for nucleic acid staining.

The molten agarose was poured into a gel tray with a comb positioned to create sample wells. After the gel solidified, the comb was removed and the tray was placed in the electrophoresis chamber. DNA samples and controls were loaded into the wells.

Electrophoresis was performed at 80 V for approximately 60 minutes, depending on the gel size and desired separation. After electrophoresis, DNA bands were visualized under UV illumination to detect any fragmentation, smearing, or alterations in band pattern compared to the control DNA sample.

RESULTS

X-ray diffraction (XRD) analysis

X-ray diffraction was used to determine the crystalline structure of the ZnO nanoparticles biosynthesized from *C. sinensis* leaves. The XRD pattern confirmed the characteristic diffraction peaks of ZnO, indicating the formation of highly crystalline nanoparticles.

The analysis revealed prominent diffraction peaks at 2θ values of 32.00°, 34.56°, 36.60°, 47.99°, 56.80°, 63.04°, and 68.14°, corresponding to the Miller indices (100), (002), (101), (102), (110), (103), and (112), respectively. These peaks are consistent with the hexagonal wurtzite structure of ZnO as documented in the Joint Committee on Powder Diffraction Standards (JCPDS card no. 800075).

These findings confirm that the synthesized ZnO NPs exhibit a well-defined crystalline structure.

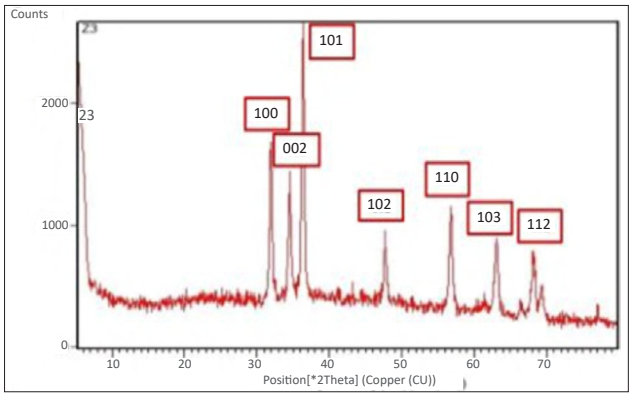

Figure 1. X-ray diffraction pattern of ZnO NPs biosynthesized from *C. sinensis* leaves

Cell viability (MTT assay)

The cytotoxic effect of ZnO nanoparticles on the HepG2 hepatocellular carcinoma cell line was assessed using the MTT assay. Cells were treated with ZnO NP concentrations of 0.5, 1, 2, and 5 µg/mL for 72 hours.

As shown in Table 1, cell viability decreased progressively with increasing ZnO NP concentration. The percentage of viable cells at each concentration was 42.13%, 38.03%, 33.56%, and 26.84%, respectively. These data demonstrate a clear dose-dependent reduction in cell viability.

The concentration of ZnO NPs required to inhibit 50% of cell proliferation (IC_{50}) was calculated as 2.87 µg/mL, indicating strong antiproliferative activity at relatively low concentrations.

Microscopic images (Figure 3) show morphological alterations characteristic of cytotoxicity, including cell shrinkage, loss of adherence, and reduced cellular density. These effects intensified with higher nanoparticle concentrations. The observed reduction in viability may be attributed to generation of reactive oxygen species (ROS), mitochondrial membrane depolarization, and subsequent activation of caspasedependent apoptotic pathways, which are well-documented mechanisms of ZnO NPinduced cytotoxicity.

Table 1. Effect of ZnO nanoparticles biosynthesized from *C. sinensis* leaves on HepG2 cell viability

	Concentration (µg/mL)				
	0	0.5	1	2	5
R1	350	128	150	112	105
R2	332	150	144	131	104
R3	361	156	126	121	87
R4	369	161	117	110	83
Mean	353	148.75	134.25	118.50	94.75
Viability (%)	100	42.14	38.03	33.57	26.84

Linear regression equation:

$$Y = -15.489x + 94.582$$

$$IC_{50} = 2.87\ \mu g/mL$$

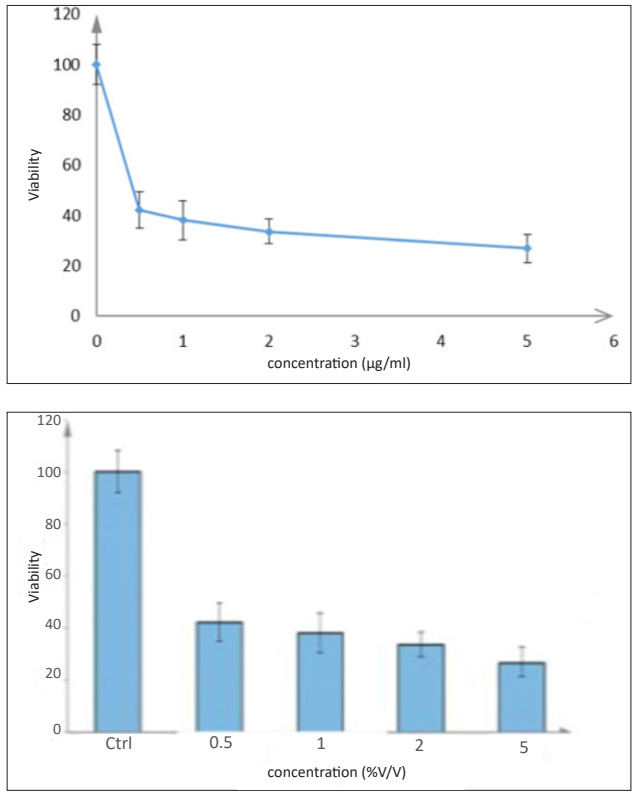

(A) Concentration in µg/mL; (B) Percentage viability (v/v)

Figure 2. Effect of different concentrations of ZnO nanoparticles biosynthesized from *C. sinensis* leaves on the viability of HepG2 cells after 72 hours of treatment

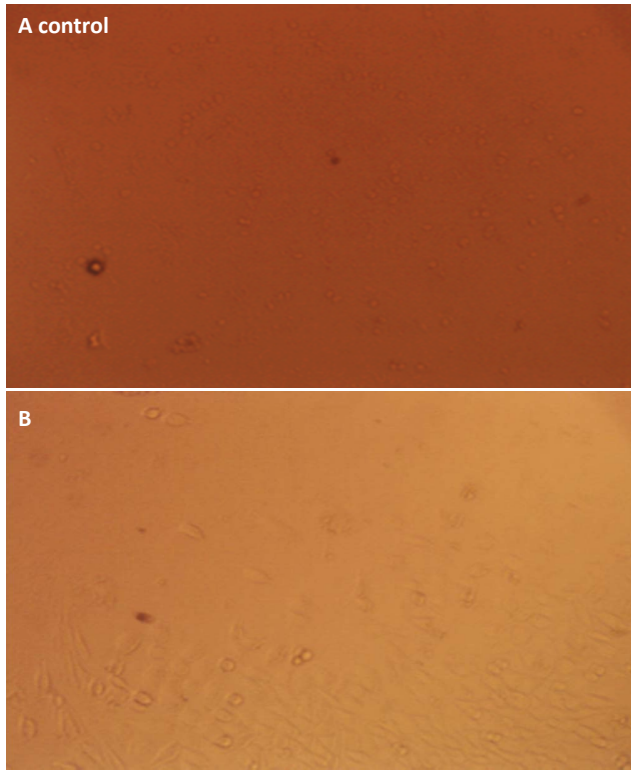

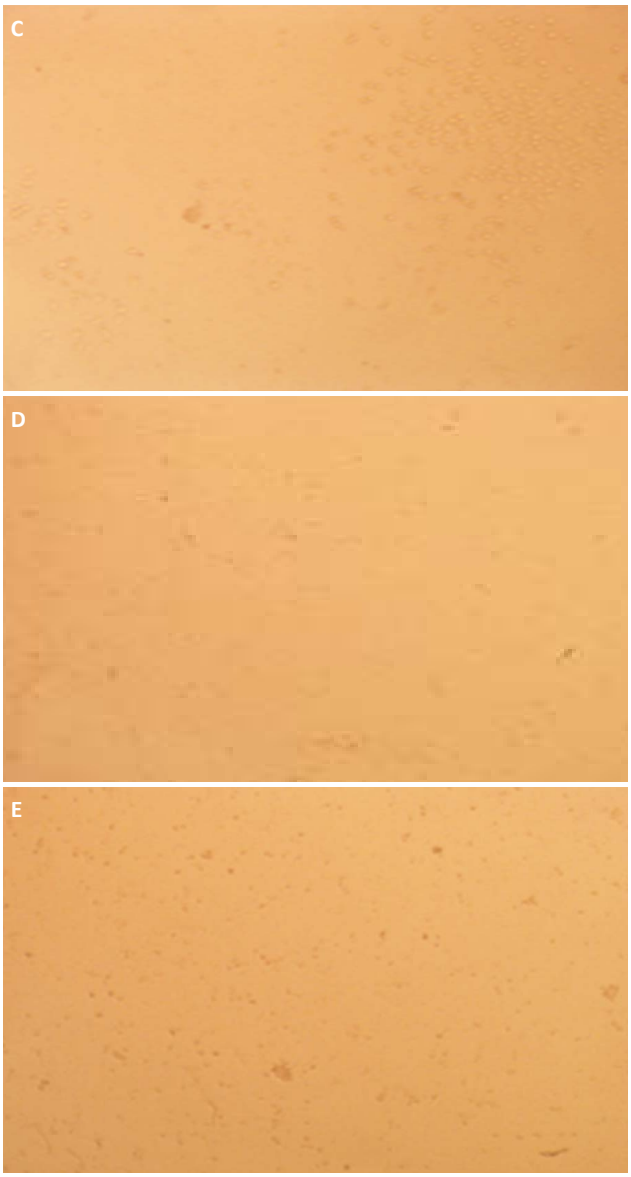

Figure 3. HepG2 cells treated with different concentrations (B-E; 0.5, 1, 2, and 5 µg/mL) of ZnO nanoparticles biosynthesized from *C. sinensis* leaves

Antioxidant activity of ZnO nanoparticles (DPPH assay)

The antioxidant capacity of the ZnO nanoparticles was evaluated using the DPPH free radical scavenging assay. The reduction of DPPH is visually indicated by a color change from dark violet to light yellow, reflecting the ability of the sample to neutralize free radicals. ZnO NPs demonstrated concentrationdependent antioxidant activity at doses of 0.12, 0.25, 0.5, and 1 µg/mL.

The increase in scavenging activity may be attributed to the availability of hydrogen atoms donated by antioxidants or the electron-transfer mechanism in which electrons move from oxygen to the nitrogen center of the DPPH molecule. As the concentration of ZnO NPs increased, the percentage of radical inhibition also increased.

The highest scavenging activity (81.627%) was recorded at 1 µg/mL, while the lowest (63.730%) was observed at 0.12 µg/mL, demonstrating a clear dose-response relationship (Table 2.)

Table 2. Antioxidant activity of ZnO nanoparticles biosynthesized from *C. sinensis* leaves using the DPPH assay

Sample	Concentration (µg/mL)	Test Result	Antioxidant activity (%)
B (Control)	—	1.7651	—
C	1.00	0.324	81.63
D	0.50	0.328	81.44
E	0.25	0.376	78.72
F	0.12	0.640	63.73

Antihemolytic properties of ZnO nanoparticles

The hemolysis assay demonstrated that ZnO nanoparticles did not induce any detectable damage or lysis of human red blood cells (RBCs) at all tested concentrations (0.12, 0.25, 0.5, and 1 µg/mL). As shown in Table 3, hemolysis levels remained 0% across all nanoparticle concentrations, in contrast to the positive control (Triton X100), which produced 100% hemolysis.

These findings indicate that ZnO NPs biosynthesized from *C. sinensis* leaves exhibit excellent hemocompatibility. The absence of RBC membrane degradation suggests their potential suitability for preventive or therapeutic biomedical applications without inducing cytotoxicity toward human erythrocytes.

Table 3. Antihemolytic properties of ZnO nanoparticles biosynthesized from *C. sinensis* leaves at different concentrations

Sample	Concentration (µg/mL)	Test Result	Hemolysis (%)
A	Positive control	2.4694	100
B	Negative control	0.3708	0
C	1.00	0.5851	0
D	0.50	0.5043	0
E	0.25	0.4950	0
F	0.12	0.4887	0

DNA fragmentation test on human DNA

Agarose gel electrophoresis was performed to assess whether ZnO NPs caused DNA fragmentation after 2 hours of incubation with human genomic DNA. The nanoparticles were tested at concentrations of 0.12, 0.25, 0.5, and 1 µg/mL.

The electrophoresis results showed no observable DNA fragmentation, smearing, or migration abnormalities across all tested concentrations (Figure 4). The DNA bands of treated samples were identical to the untreated control sample, indicating that ZnO nanoparticles biosynthesized

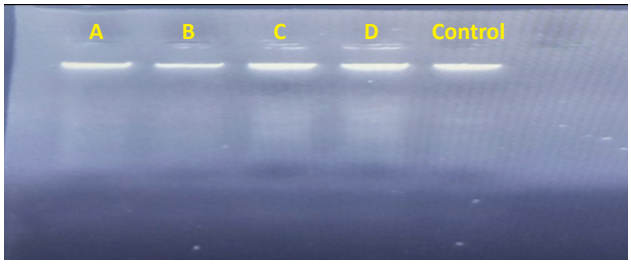

Figure 4. Demonstration of the DNA electrophoresis process and the absence of fragmentation using different concentrations of ZnO NPs (A, B, C, and D): 0.12 µg/mL, 0.25 µg/mL, 0.5 µg/mL, and 1 µg/mL

from *C. sinensis* leaves do not induce structural damage to human DNA under the tested conditions.

These findings support the non-genotoxic nature of the nanoparticles and further reinforce their potential biosafety for biomedical applications.

DISCUSSION

Xray diffraction (XRD) analysis

The XRD analysis of ZnO nanoparticles biosynthesized from *C. sinensis* leaves revealed a diffraction pattern within the 2θ range of 10°-80°. The observed peaks at 32.00°, 34.56°, 36.60°, 47.99°, 56.80°, 63.04°, and 68.14° correspond to the Miller indices (100), (002), (101), (102), (110), (103), and (112), respectively. These reflections indicate the presence of a hexagonal wurtzite crystalline structure, which aligns with standard data from the Joint Committee on Powder Diffraction Standards (JCPDS card no. 800075).

The diffraction peaks confirmed the formation of crystalline ZnO nanoparticles, consistent with previous reports [26-29]. Studies by researchers such as [30] and [31], who synthesized ZnO nanoparticles using strawberry waste extract and celery leaf extract, respectively, also reported comparable diffraction patterns. This consistency with the existing literature reinforces the reliability of the biosynthesis process used in this study.

The sharp and welldefined peaks observed in the XRD profile indicate a high degree of crystallinity and the absence of notable agglomeration among the nanoparticles. This suggests uniform particle distribution and nanoscale dimensions, which improve the ability of ZnO NPs to interact with cellular membranes. Due to their small size and crystalline nature, these nanoparticles may exhibit enhanced biological activity, making them promising candidates for preventive or therapeutic applications.

Cell viability (MTT assay)

The in vitro cytotoxicity assessment conducted on HepG2 cells demonstrated a clear dose-dependent decrease in cell viability following 72 hours of exposure to ZnO nanoparticles biosynthesized from *C. sinensis* leaves. The viability percentages observed at concentrations of 0.5, 1, 2, and 5 µg/mL were 42.13%, 38.03%, 33.56%, and 26.84%, respectively, confirming the inhibitory effect of ZnO NPs on HepG2 cell proliferation. As illustrated in Figures 1 and 2, the reduction in viable cells corresponds to increased nanoparticle concentration, suggesting enhanced nanoparticle-cell interactions [32].

The anticancer potential of the biosynthesized nanoparticles may partially be attributed to the phytochemical constituents of *C. sinensis*. Notably, the extract contains vitamin E, a potent antioxidant known for its protective and modulatory effects on cellular oxidative stress. While vitamin E generally acts as a free radical scavenger, its presence in the synthesis medium may influence nanoparticle formation, stability, or interaction with cancer cells. Moreover, the inherent selective toxicity of ZnO nanoparticles toward malignant cells likely contributes to the observed IC_{50} value of 2.87 µg/mL, reflecting strong antiproliferative activity at low concentrations.

The findings of this study align with previous reports. Research conducted in [33] demonstrated that prolonged exposure to ZnO NPs at concentrations above 25 µg/mL significantly reduced the viability of human umbilical vein endothelial (HUVEC) cells. Similarly, studies by [34] and [35] reported substantial decreases in cell viability in human epidermoid carcinoma A431 cells and HepG2 cells, respectively, when treated with ZnO NPs synthesized from plant extracts such as *Euphorbia retusa*. In the latter study, an IC_{50} value of 25.6 µg/mL was reported, further supporting the cytotoxic potential of phytogenic ZnO nanoparticles.

The underlying mechanism of ZnO NPinduced cytotoxicity is widely attributed to oxidative stress-mediated apoptosis. ZnO nanoparticles are known to release Zn^{2+} ions, which promote electrostatic interactions between the nanoparticle surface and negatively charged components of the cancer cell membrane. This interaction facilitates the generation of reactive oxygen species (ROS), including superoxide anion ($O_2^{\bullet -}$), hydroxyl radicals (•OH), and hydrogen peroxide (H_2O_2) under oxidative stress conditions [36,37]. These ROS species can disrupt mitochondrial membrane potential, activate caspase cascades, and ultimately trigger programmed cell death.

Based on these observations, the present study concludes that the anticancer activity of ZnO nanoparticles biosynthesized from *C. sinensis* leaves is predominantly mediated through ROS generation and oxidative stress, leading to apoptosis in HepG2 liver cancer cells.

Antioxidant activity of ZnO nanoparticles (DPPH assay)

The antioxidant potential of the ZnO nanoparticles was evaluated using the DPPH free radical scavenging assay, a simple and reliable technique commonly used to assess the electron-donating and hydrogendonating capacity of nanoparticles and plantderived compounds [38]. As shown in Table 2, the percentage of DPPH radical scavenging increased progressively with the concentration of ZnO NPs. The highest scavenging activity (81.627%) was observed at 1 µg/mL, indicating that the biosynthesized ZnO nanoparticles possess significant antioxidant capacity.

The characteristic color change from deep violet (control DPPH solution) to yellow reflects the reduction of DPPH radicals. This reaction occurs when antioxidants donate hydrogen atoms or electrons to DPPH, converting the unstable free radical into a stable, nonradical form. The reaction mechanism may involve hydrogen atom transfer (HAT) or single-electron-transfer (SET) processes, where electron density is shifted from oxygen toward the nitrogen center of the DPPH molecule [39-41]. The pronounced color change observed in this study therefore supports the active participation of ZnO NPs in radical neutralization.

The present study's findings align with prior reports. For example, [42] demonstrated that ZnO nanoparticles synthesized using *Azadirachta indica* leaf extract exhibited enhanced radical scavenging activity, with increasing concentration correlating with greater antioxidant potential. Similarly, studies reported in [43] and [44] showed that ZnO nanoparticles biosynthesized from *Capsicum chinense* fruit extract exhibited superior antioxidant and anticancer activity

compared to conventionally synthesized ZnO NPs. These findings collectively confirm that phytogenic synthesis enhances the antioxidant properties of ZnO nanoparticles, likely due to the presence of polyphenols, flavonoids, and other bioactive compounds from plant extracts adhered to the nanoparticle surface.

Taken together, the results support the conclusion that ZnO nanoparticles synthesized using *C. sinensis* leaves exhibit strong antioxidant activity with a clear dose-dependent increase in free radical scavenging. This antioxidant potential contributes to their broader biomedical relevance, including possible roles in mitigating oxidative stress, reducing cellular damage, and complementing anticancer mechanisms.

Antihemolytic properties of ZnO nanoparticles

The hemolysis assay results demonstrated that ZnO nanoparticles did not induce measurable degradation or lysis of human red blood cells (RBCs) at any of the tested concentrations (0.12, 0.25, 0.5, and 1 μg/mL), as shown in Table 3. Hemolysis remained at 0% for all ZnO NP treatments, whereas the positive control exhibited 100% hemolysis, confirming the specificity and sensitivity of the assay.

These findings are consistent with reports from previous studies [45,46], which demonstrated that ZnO nanoparticles synthesized from various plant extracts, such as *Allium cepa*, *Asparagus racemosus*, and *Citrus limon*, did not induce hemolysis in RBCs when tested alongside MCF7 and HeLa cell lines. Similar observations were reported in studies [47,18], where ZnO NPs and biocomplexes synthesized using *Lagerstroemia indica* were found to exhibit anticancer potential without causing erythrocyte membrane damage.

Collectively, these results suggest that ZnO NPs synthesized from *C. sinensis* leaves are highly hemocompatible and do not induce structural damage to human erythrocytes even at the highest concentrations tested. This property supports their potential use as anticancer agents, particularly at low therapeutic doses where systemic toxicity must be minimized [48].

Fragmentation test on human DNA

The absence of DNA damage at the concentrations used in the study indicates that ZnO NPs did not induce detectable DNA damage under the tested conditions. These findings are consistent with those of previous studies [49,50], which found that the ZnO NPs/Rr protected human DNA from damage caused by H_2O_2 photolysis, and with those of another study [51], which found that the inhibitory effect of DNA damage increased with increasing concentration.

CONCLUSIONS

Zinc oxide nanoparticles (ZnO NPs) showed high efficacy in inhibiting the viability of human liver cancer cells after a 72-hour incubation period. Even though the concentrations used were very low, they did not cause hemolysis or affect human DNA. ZnO NPs also showed high efficacy in removing free radicals generated in cells.

ORCID iDs

Halah Al-Luhaiby https://orcid.org/0009-0007-4464-8473
Jabbar Abadi Mohammed https://orcid.org/0000-0002-6778-8643

REFERENCES

1. Jawad D. Incidence and histopathology of hepatocellular carcinoma in Iraqi patients. *Cent Asian J Med Nat Sci.* 2023;4(4):40-45.
2. Addissouky TA, Sayed IETE, Ali MM, Wang Y, Baz AE, Khalil AA, Elarabany N. Latest advances in hepatocellular carcinoma management and prevention through advanced technologies. *Egypt Liver J.* 2024;14(1):2.
3. Peng X, Pan Q, Zhang B, Wan S, Li S, Luo K, et al. Highly stable coordinated polymeric nanoparticles loading copper(II) diethyldithiocarbamate for combinational chemo/chemodynamic therapy of cancer. *Biomacromolecules.* 2019;20(6):2372-2383. https://doi.org/10.1021/acs.biomac.9b00690.
4. Feng C, Yuan X, Chu K, Zhang H, Ji W, Rui M. Preparation and optimization of poly(lactic acid) nanoparticles loaded with fisetin to improve anticancer therapy. *Int J Biol Macromol.* 2019;125:700-710. https://doi.org/10.1016/j.ijbiomac.2018.12.228.
5. Yin W, Mao C, Luan X, Shen DD, Shen Q, Su H, et al. Structural basis for inhibition of the RNA-dependent RNA polymerase from SARS-CoV-2 by remdesivir. *Science.* 2020;368(6498):1499-1504. https://doi.org/10.1126/science.abc1560.
6. Chen S, Wu J, Tang Q, Xu C, Huang Y, Huang D, et al. Nano micelles based on hydroxyethyl starch-curcumin conjugates for improved stability, antioxidant and anticancer activity of curcumin. *Carbohydr Polym.* 2020;228:115398.
7. Nejabat A, Emamat H, Afrashteh S, Jamshidi A, Jamali Z, Farhadi A, et al. Association of serum 25 hydroxyvitamin D status with cardiometabolic risk factors and total and regional obesity in southern Iran: evidence from the PoCOsteo study. *Sci Rep.* 2024;14(1):17983. https://doi.org/10.1038/s41598-024-68773-1.
8. Huston M, DeBella M, DiBella M, Gupta A. Green synthesis of nanomaterials. *Nanomaterials* (Basel). 2021;11(8):2130. https://doi.org/10.3390/nano11082130.
9. Rahaman MM, Islam T. Anticancer activity of plant derived compounds: a literature based review. *Clin Oncol.* 2022;7:1917.
10. Miyata K, Kaneko T, Morikawa Y, Sakakibara H, Matsushima T, Misawa M, et al. Efficacy and safety of intravenous immunoglobulin plus prednisolone therapy in patients with Kawasaki disease (Post RAISE): a multicentre, prospective cohort study. *Lancet Child Adolesc Health.* 2018;2(12):855-862.
11. Verma R, Pathak S, Srivastava AK, Prawer S, Tomljenovic Hanic S. ZnO nanomaterials: green synthesis, toxicity evaluation, and new insights into biomedical applications. *J Alloys Compd.* 2021;876:160175. https://doi.org/10.1016/j.jallcom.2021.160175.
12. Batool S, Sohail S, Ud Din F, Alamri AH, Alqahtani AS, Alshahrani MA, et al. A detailed insight into tumor targeting using nanocarrier drug delivery systems. *Drug Deliv.* 2023;30(1):2183815. https://doi.org/10.1080/10717544.2023.2183815.
13. Sengul AB, Asmatulu E. Toxicity of metal and metal oxide nanoparticles: a review. *Environ Chem Lett.* 2020;18:1659-1683.
14. Gavas S, Quazi S, Karpiński TM. Nanoparticles for cancer therapy: current progress and challenges. *Nanoscale Res Lett.* 2021;16(1):173.
15. Elumalai K, Srinivasan S, Shanmugam A. Review of the efficacy of nanoparticle based drug delivery systems for cancer treatment. *Biomed Technol.* 2024;5:109-122.
16. Canta M, Cauda V. Investigation of the parameters affecting ZnO nanoparticle cytotoxicity behaviour: a tutorial review. *Biomater Sci.* 2020;8(22):6157-6174.
17. Naser SS, Ghosh B, Simnani FZ, Singh D, Choudhury A, Nandi A, et al. Emerging trends in the application of green synthesized biocompatible ZnO nanoparticles for a translational paradigm in cancer therapy. *J Nanotheranostics.* 2023;4(3):248-279.
18. Mthana MS, Mthiyane MN, Ekennia AC, Singh M, Onwudiwe DC. Cytotoxicity and antibacterial effects of silver doped zinc oxide nanoparticles prepared using Capsicum chinense fruit extract. *Sci Afr.* 2022;17:e01365.

19. Supin KK, PM PN, Vasundhara M. Enhanced photocatalytic activity of ZnO nanoparticles developed using Lepidagathis ananthapuramensis leaf extract. *RSC Adv.* 2023;13(3):1497-1515.
20. Azhar NA, Bakar SAA, Ngalim SH, Ahmad NH. Cellular uptake of Catharanthus roseus silver nanoparticles in human hepatocellular carcinoma HepG2 cells. *Malays J Med Health Sci.* 2023;19(4):171-177. https://doi.org/ 10.47836/mjmhs19.4.26.
21. Ahmadian E, Babaei H, Nayebi AM, Eftekhari A, Eghbal MA. Mechanistic approach to the toxic effects of bupropion in primary rat hepatocytes. *Drug Res* (Stuttg). 2017;67(4):217-222.
22. Kumara P, Sunil K, Arun Kumar B. Determination of DPPH free radical scavenging activity by RP HPLC: rapid sensitive method for the screening of berry fruit juice freeze dried extract. *Nat Prod Chem Res.* 2018;6(5):341. https://doi.org/10.4172/2329-6836.1000341.
23. Brusini R, Tran NLL, Cailleau C, Domergue V, Nicolas V, Dormont F, et al. Assessment of squaleneadenosine nanoparticles in two rodent models of cardiac ischemia-reperfusion. *Pharmaceutics*. 2023;15(7):1790.
24. Jose GP, Santra S, Mandal SK, Sengupta TK. Singlet oxygen mediated DNA degradation by copper nanoparticles: potential towards cytotoxic effects on cancer cells. *J Nanobiotechnol.* 2011;9:1-8.
25. Wittmeier P, Hummel S. Agarose gel electrophoresis to assess PCR product yield: comparison with spectrophotometry, fluorometry, and qPCR. *Biotechniques.* 2022;72(4):155-158.
26. Muhammad W, Ullah N, Haroon M, Abbasi BH. Optical, morphological, and biological analysis of zinc oxide nanoparticles using Papaver somniferum L. *RSC Adv.* 2019;9(51):29541-29548.
27. Hassan HMA, Alhumaimess MS, Alsohaimi IH, Essawy AA, Hussein MF, Alshammari MH, et al. Biogenic mediated synthesis of Cs_2O-MgO/MPC nanocomposite for biodiesel production from olive oil. *ACS Omega.* 2020;5:27811-27822.
28. Thi TUD, Nguyen TT, Thi YD, Ta Thi KH, Phan BT, Pham KN. Green synthesis of ZnO nanoparticles using orange fruit peel extract for antibacterial activity. *RSC Adv.* 2020;10:23899-23907.
29. Takele E, Bogale RF, Shumi G, Kenasa G. Green synthesis, characterization, and antibacterial activity of CuO/ZnO nanocomposite using Zingiber officinale rhizome extract. *J Chem.* 2023;2023:3481389.
30. Khan AU, Malik N, Singh B, Ansari NH, Rehman M, Yadav A. Biosynthesis and characterization of zinc oxide nanoparticles obtained from strawberry waste extract. *J Umm Al Qura Univ Appl Sci.* 2023;9(3):268-275.
31. Al Ogaili FH, Almahdawi FH. Green fabrication and characterization of zinc oxide nanoparticles using celery leaf extract. *J Surv Fish Sci.* 2023;10(4 Suppl):2938-2945.
32. Weiss G, Schaible UE. Macrophage defense mechanisms against intracellular bacteria. Immunol Rev. 2015;264(1):182-203.
33. Poier N, Hochstöger J, Hackenberg S, Scherzad A, Bregenzer M, Schopper D, et al. Effects of zinc oxide nanoparticles in HUVECs: cyto and genotoxicity and functional impairment after long term and repetitive exposure *in vitro*. *Int J Nanomedicine.* 2020;15: 4441-4452.
34. Al Muhana WHY, Alaridhi JAM. Protective role of nano extract of Cordia myxa fruits against indomethacin induced renal toxicity in male rats. *J Chem Health Risks.* 2023;13(4):158-165.
35. Khan MJ, Ahmad A, Khan MA, Siddiqui S. Zinc oxide nanoparticles induce apoptosis in human epidermoid carcinoma cells through reactive oxygen species generation and DNA degradation. *Biol Trace Elem Res.* 2021;199:2172-2181.
36. Alqahtani AS, Ullah R, Shahat AA. Bioactive constituents and toxicological evaluation of selected antidiabetic medicinal plants of Saudi Arabia. *Evid Based Complement Alternat Med.* 2022;2022:7123521. https://doi.org/10.1155/2022/7123521.
37. Abar ES, Alaridhi JA. Effect of aqueous extract of Zingiber officinale Roscoe on the histological structure of the prostate gland of male white rabbits (Oryctolagus cuniculus). *Plant Arch.* 2019;19:293-298.
38. Mushattat SJ, Alaridi JA, Hassan AB. Histological changes in the placenta and selected physiological effects in aborted women infected with Toxoplasma gondii. *Ann Biol.* 2020;36(1):22-25.
39. Fan J, Liu X, Pan W, Douglas MW, Bao S. Epidemiology of coronavirus disease in Gansu Province, China, 2020. *Emerg Infect Dis.* 2020;26(6):1257.
40. Gassim FAZG, Makkawi AJJ. Anticancer activity of synthesized ZnO and ZnO/AgCl nanocomposites against five human cancer cell lines. *Indones J Chem.* 2023;23(2):333-340.
41. Mushattat SJ, Al Hadraawy SK, Mohammed JA. Effect of magnetized water on reducing histological and physiological alterations induced by Ascaridia galli infection in domestic chickens. *J Glob Pharma Technol.* 2018;10(1):97-103.
42. Khorrami S, Zarepour A, Zarrabi A. Green synthesis of silver nanoparticles at low temperature with enhanced DPPH radical scavenging and selective cytotoxicity against MCF 7 and BT 20 tumor cell lines. *Biotechnol Rep* (Amst). 2019;24:e00393.
43. Mohammad JE, Hasnawi NM. Effect of ciprofloxacin on the histological structure of the ovary in albino rabbits. *J Glob Pharma Technol.* 2018;10(3):498-508.
44. Sujitha V, Murugan K, Paulpandi M, Panneerselvam C, Suresh U, Roni M, et al. Green synthesized silver nanoparticles as a novel control tool against dengue virus (DEN 2) and its primary vector Aedes aegypti. *Parasitol Res.* 2015;114:3315-3325.
45. Al Aamelia MH, Al Qazwini YM, Mohammed JA. Histological investigation of the effects of cinnamon extract on the skin of male sheep affected by mange. *Syst Rev Pharm.* 2020;11(12):380-386.
46. Awan SS, Khan RT, Mehmood A, Hafeez M, Abass SR, Nazir M, Raffi M. Ailanthus altissima leaf extract mediated green synthesis of zinc oxide nanoparticles for antibacterial and antioxidant activity. *Saudi J Biol Sci*. 2023;30(1):103487.
47. Ansari A, Ali A, Khan N, Umar MS, Owais M. Synthesis of steroidal dihydropyrazole derivatives using green ZnO nanoparticles and evaluation of their anticancer and antioxidant activities. *Steroids*. 2022;188:109113.
48. Salem MSED, Mahfouz AY, Fathy RM. Assessment of antibacterial and antihemolytic activities of zinc oxide nanoparticles synthesized using plant extracts and gamma irradiation against uropathogenic multidrug resistant *Proteus vulgaris*. *Biometals*. 2021;34:175-196.
49. Behera A, Awasthi S. Anticancer, antimicrobial, and hemolytic assessment of zinc oxide nanoparticles synthesized from *Lagerstroemia indica*. *BioNanoScience.* 2021;11(4):1030-1048.
50. Meydan I, Burhan H, Gür T, Seçkin H, Tanhaei B, Sen F. Characterization of Rheum ribes derived zinc oxide nanoparticles and their antidiabetic, antibacterial, DNA damage prevention, and lipid peroxidation inhibitory activities in vitro. *Environ Res.* 2022;204:112363.
51. Gur T, Meydan I, Seckin H, Bekmezci M, Sen F. Green synthesis, characterization, and bioactivity of biogenic zinc oxide nanoparticles. *Environ Res.* 2022;204:111897.